Traps Formation and Characterization in Long-Term Energy Storing Lu2O3:Pr,Hf Luminescent Ceramics

Journal:	*The Journal of Physical Chemistry*
Manuscript ID:	Draft
Manuscript Type:	Article
Date Submitted by the Author:	n/a
Complete List of Authors:	Wiatrowska, Aneta; University of Wroclaw, Faculty of Chemistry Zych, Eugeniusz; University of Wroclaw, Faculty of Chemistry

Traps Formation and Characterization in Long-Term Energy Storing Lu_2O_3:Pr,Hf Luminescent Ceramics

ANETA WIATROWSKA[1], *EUGENIUSZ ZYCH*[1,2]*

[1] Faculty of Chemistry, University of Wroclaw, 14 F. Joliot-Curie Street

50-383 Wroclaw, Poland

[2] Wroclaw Research Centre EIT+, 147/149 Stablowicka Street

54-066 Wroclaw, Poland

KEYWORDS. Storage phosphor, defects, traps, lutetium oxide

ABSTRACT. Sintered ceramics of Lu_2O_3:Pr,Hf storage phosphor were prepared and their spectroscopic properties were evaluated. It was shown that during irradiation with X-rays as well as with short UV radiation, the material was able to accumulate energy, which could thereafter be recovered by thermal stimulation in the range of approximately 20-450 °C. The glow curve consisted of three bands peaking around 130 °C, 250 °C and 340 °C, and each of them contained two overlapping components. The thermoluminescence was found to follow the first-order kinetics mechanism and the activation energies of the traps derived from the glow curve fitting covered the range of about 0.8-2.1 eV. Frequency factors of the traps were also calculated and were mostly found to exceed the Debye frequency by 3-4 orders of magnitude indicating a

complex mechanism of the process. The fading measured nine months after the material irradiation revealed only about 30% loss of the thermoluminescence intensity. Controlled thermal annealing at defined temperatures as well as optical stimulation with infrared (980 nm, 780 nm) or violet photons (400 nm) proved that it is possible to recover the stored energy either from all traps simultaneously or just from a fraction of them leaving energy stored in the others unaffected. Irradiation with X-rays altered absorption spectrum inducing a new broad band component covering near-UV-blue-green region which perfectly harmonized with a significant decrease of absorption efficiency in the short-UV wavelengths range of f→d Pr^{3+} transitions. These variations were fully reversible by means of thermal or UV (400 nm) bleaching. Defects responsible for the energy storing were identified. Long term energy storing traps giving the high temperature TL components were assigned to the presence of Hf(IV) (electron trap), which replaced Lu(III) in the host (TL around 250 °C) and Pr^{3+} activator trapping a hole (TL around 340 °C). The good long term stability of the thermoluminescence signal and high efficiency of absorption of ionizing radiation due to a very high density of the lutetia host may make the Lu_2O_3:Pr,Hf composition an interesting material for high energy particles dosimetry.

INTRODUCTION

Mechanisms of various processes related to photoluminescence have been well understood in XX century and now we can benefit from that knowledge anticipating spectroscopic properties of various compositions and consequently we can quite deliberately design new phosphors. However, persistent and storage phosphors are not so well understood yet.[1-4] These materials can store energy trapping excited carriers in defects for hours (persistent phosphors) or days and even years (storage phosphors). Fortunately, recently we got an important tool to foresee and predict properties of such materials too, as Dorenbos combined the possibility of positioning the

electronic levels of lanthanides ions within a host forbidden energy gap with the prediction of the trap depths created by these ions.[5-9] First proofs of the applicability of this approach have recently been reported.[7-9] However, there are materials which store energy and produce efficient thermoluminescence well above room temperature due to traps created by different types of impurities, d-elements or closed-shell elements. The old, well known group of ZnS-based persistent phosphors is a good example of such a situation.[10,11]

In recent years, exploiting Lu_2O_3 host to make luminescent materials we found a group of compositions able to show a surprisingly efficient, hours-lasting persistent luminescence (Lu_2O_3:Tb,M, where M=Ca, Sr, Ba)[12,13] or being able to store energy even more permanently in yet deeper traps (Lu_2O_3:Tb,Hf).[14,15] We showed that introducing a spectroscopically inert (closed-shell), aliovalent co-dopant and adjusting the parameters of materials fabrication, formation of traps able to store energy can thus be accomplished and their properties can be controlled.

First, scant information on energy storing in Lu_2O_3:Pr,Hf ceramics we gave previously in a conference paper.[15] Here we present a comprehensive picture of the properties of Lu_2O_3:Pr,Hf as a storage phosphor with bright red luminescence due to Pr^{3+} dopant. We also present and discuss the effect of Hf co-dopant on shaping the material behavior. The Lu_2O_3:Pr,Hf ceramics can store energy acquired either upon irradiation with X-Rays or high-energy UV photons. Due to its high density (9.4 g/cm^3) and high absorption coefficient for X- and γ-Rays Lu_2O_3:Pr,Hf might be considered a good candidate for dosimeters to monitor such particles dosage in some circumstances.[16] Yet, at present, the understanding of the co-operative effect of the two co-dopants in transferring lutetia into efficient storage phosphor is most important and truly intriguing.

SAMPLE PREPARATION

Lu_2O_3:Pr,Hf sintered ceramics were made by high-temperature sintering of raw powders prepared by the Pechini technique.[17] To prepare the latter, lutetium(III) nitrate pentahydrate ($Lu(NO_3)_3 \cdot 5H_2O$, 4N), praseodymium(III) nitrate hexahydrate ($Pr(NO_3)_3 \cdot 6H_2O$, 4N), and hafnium(IV) chloride ($HfCl_4$, 3N) were used. Their stoichiometric amounts were dissolved in 2M citric acid (HOOC-CH_2-C(OH)(COOH)-CH_2-COOH) to complex the metal ions. Next, some ethylene glycol ($C_2H_4(OH)_2$) was added. The resultant solution was condensed at 80 °C and then the temperature was slowly increased up to 700 °C, which appeared sufficient to burn off the organics. For sintering, such a raw powder was pressed into a pellet 8 mm in diameter under the load of 4 tons. Such a pellet was transferred into a tube furnace and was heated at 1700 °C for 5 hours under a reducing atmosphere – a mixture of 75%N_2-25%H_2. The concentrations of praseodymium and hafnium in Lu_2O_3:Pr,Hf ceramics reported here were 0.05% and 0.1%, respectively. During the course of our research such a composition was found to give the most intense thermoluminescence. Details of the composition optimization are not presented in this paper.

EXPERIMENTAL METHODS

The samples' phase purity was evaluated by powder X-Ray diffraction technique using D8 Advance X-Ray diffractometer from Bruker with Nickel-filtered Cu $K_{\alpha 1}$ radiation (λ=1.540596 Å). The measurement was performed in the range of 2θ=10-120 degree with the step of 2θ=0.00857 degree and the counting time of 0.2 s per point.

The luminescence excitation spectra were measured in the range of 250-600 nm at room temperature with an FSL 920 Spectrometer from Edinburg Instruments using a 450W Xenon

lamp as an excitation source. These spectra were recorded on freshly prepared specimen as well as on material with different history: treated with X-rays, and further irradiated with 400 nm radiation. The 632 nm luminescence decay traces at elevated temperatures (25-500 °C) were measured using the third harmonic (355 nm) of the YAG:Nd laser as an excitation source and PMT R928P side-on type photomultiplier as a detector. Emission and excitation spectra (in the range of 50-333 nm) were also recorded at room temperature (RT) using synchrotron radiation at the Superlumi station of Hasylab (DESY, Hamburg, Germany). The sodium salicylate was used as a standard to correct excitation spectra for the incident radiation intensity. Emission spectra were corrected for the recording system characteristics. Absorption spectra were obtained using Cary 5000 SCAN UV-VIS-NIR spectrophotometer. Thermoluminescence (TL) glow curves were recorded using a custom-made temperature controller with linear heating rate in the range of 20-500 °C and using Ocean Optics HR2000 CG spectrometer operating under Spectra Suit dedicated software. The light produced upon heating was collected with a 74-UV lens coupled to a QP600-1-SR waveguide which transferred it to the detector. TL glow curves were recorded with the counting time of 1 s and monitoring the intensity of the Pr^{3+} red emission band around 630 nm. The setup allowed to record full spectra in the range of 200-1100 nm, simultaneously. The typical heating rate was 4.8 °C/s. Additionally, a set of glow curves was recorded varying the heating rate in the range of 1-8 °C/s. The glow curves were deconvoluted into TL components using GlowFit software kindly supplied by Dr. M. Puchalska from Cracow, Poland.[18] White X-Rays from a Cu lamp of DRON-1 diffractometer were used for irradiation of the materials prior to thermoluminescence and optically stimulated luminescence (OSL) experiments. Only to monitor fading of the TL signal irradiations were performed with 254 nm, as it allowed to control the dosage to a much higher degree than using an X-ray machine. The

OSL measurements were done upon stimulation with 980 nm or 780 nm radiation from 1 mW diode lasers and with 400 nm radiation from a semiconductor diode. The Kröger-Vink notation of defects was used throughout the paper.[19,20]

RESULTS

All XRD patterns perfectly agreed with the cubic structure of Lu_2O_3 (ICSD#40471),[21] indicating that the synthesized products are crystalline and single phase at least to the detection limit of this technique. These findings shall not be presented here, as analogous results for Lu_2O_3 powders and ceramics were frequently published in recent years.[22-24]

Figure 1 presents TL glow curves of undoped Lu_2O_3, singly doped Lu_2O_3:0.05%Pr, Lu_2O_3:0.1%Hf and doubly activated Lu_2O_3:0.05%Pr,0.1%Hf ceramics measured immediately after irradiation of the materials with X-Rays. In the undoped lutetia as well as in the composition containing solely Hf dopant, no TL signal was observed. Single activation with Pr allowed getting TL located around 340 °C of barely recordable intensity. Simultaneous co-doping with Pr and Hf changed the situation completely and a very intense red thermoluminescence appearing at three different ranges of temperatures, around 135 °C, 250 °C and 340 °C, was seen. Hence, it is clearly a *cooperative* effect of both Pr and Hf introduced into the Lu_2O_3 host lattice, which transforms the composition into efficient storage phosphor.

Figure 2 presents excitation spectra of the 610 nm and 631.5 nm emissions together with photoluminescence and thermoluminescence (at 250 °C) spectra of Lu_2O_3:0.05%Pr,0.1%Hf ceramics. The excitation spectra of the Pr^{3+} emissions is dominated by broad bands around 300 nm resulting from the 4f→5d absorption of Pr^{3+} as already identified in[25]. It is well seen that monitoring the two different wavelengths (610 nm and 631.5 nm) quite noticeable differences in

the ratio of the f→d components around 280 nm and 320 nm appear. This indicates that Pr occupies both C_2 and C_{3i} sites offered by the lutetia host.[25] At wavelengths shorter than approximately 220 nm the incident photons are absorbed by the host lattice through its fundamental absorption band. The narrow peak at 218 nm reflects presumably the formation of free exciton while at yet shorter wavelengths the energy is sufficient to raise electrons to the conduction band and thus forming free carriers, electrons and holes. Analogous effects in excitation spectra were observed and analyzed in detail for Lu_2O_3:Eu.[26] Under the excitation into the $4f^2 \rightarrow 4f5d$ transition, the ceramics produce strong luminescence in the range of 590 - 700 nm and much less intense emission covering the range of 700 - 770 nm. Both structures were assigned by De Mello Donega to the $^1D_2 \rightarrow {}^3H_4$ and $^1D_2 \rightarrow {}^3H_5$ transitions, respectively.[25] Practically, no emission from the higher positioned $^3P_0$ level is observed. The TL emission spectrum (blue line, right hand side in Figure 2) appears very similar to the PL (black line). Some small variations in relative intensities of the components may well result from the different temperatures of both experiments as well as from altered ratio of the emissions from Pr(C_2) and Pr(C_{3i}) ions.

The Lu_2O_3:Pr,Hf ceramics showed some small red afterglow, both after exposure into short UV radiation (<330 nm) and into X-Rays. Figure 3 presents TL glow curve recorded in the range of 323-773 K (50-500 °C) and its deconvolution into six components. The experimental glow curve contains three main bans peaking around 137 °C, 250 °C and 340 °C. All the bands are asymmetrically broadened from the low-temperature side to some extent. Assuming the first-order kinetics, the whole glow curve could be deconvoluted into six components, according to eq 1:

$$I(t) = -\frac{dn}{dt} = sn \exp\left(-\frac{E}{kT}\right), \quad (1)$$

where *I(t)* corresponds to TL intensity in photons per second at time *t* during the heating, *s* (s^{-1}) is a frequency factor (with typical values being in the range of 10^{12}-10^{14} s^{-1}, the Debye frequency) and *E* stands for the trap depth.[27] The parameters of the six traps derived from the fitting with the first-order kinetics are listed in Table 1.

One can note that the highest-temperature TL glow band has the most symmetric shape. Consequently, one could consider that it results from a second-order kinetic process.[1] Indeed, we were able to make a good accuracy fit in which this constituent of the glow curve could be reproduced as one component of second-order kinetics with E = 2.25 eV and $s = 1\times10^{11}s^{-1}$. However, the later results, especially the variations of the TL glow bands with varying doses, which will be presented in Figure 4, disproved such supposition and therefore we consider the high temperature TL glow component to result from two traps of first-order kinetics.

Traps #1 contributes almost exclusively to the TL band peaking around 135°C. Trap #2 gives TL of negligible intensity around 180 °C. Traps #3 and #4 compose together the TL band around 250 °C, which is the most intense among the three, and finally carriers from traps #5 and #6 are responsible for the TL appearing around 340 °C. Hence, in fact each of the three bands (and certainly the two located at higher temperatures) seems to be composed of two components representing two traps characterized by pretty close depths (see Table 1). This might be connected with the structure of the Lu_2O_3 host material in which two symmetry sites, C_2 and C_{3i}, for metal cations are present.[25,26] This is, however, just an intuitive suspicion at present, having no real experimental support.

Frequency factor is a parameter whose value may give some indications on the mechanism of the TL process.[27] In a typical TL course, when trapped electron is moved to conduction band and after some diffusion falls into the emitting center to radiatively recombine there, *s* is on the order

of 10^{13} s^{-1}. The data in Table 1 prove that in the case of Lu_2O_3:Pr,Hf the values of frequency factors for most of the traps are by about 3-4 orders of magnitude larger. Noticeably higher frequency factors are usually connected with a more complex mechanism of the process. Mandowski showed that in such cases cascade detrapping may appear a probable mechanism.[28] Enhanced values of the frequency factor may also result from parallel happening courses. On the other hand, in the case of strongly overlapping TL bands the parameters from fits should not be treated as definitive.[27]

Knowing the trap depth and its associated frequency factor an average time a carrier spends in the trap (τ) can be calculated according to eq 2[27]:

$$\tau = s^{-1} \exp(\frac{E}{kT}) \quad (2)$$

These values are also listed in Table 1 and show that traps producing the TL bands at 250 °C and 340 °C (#3-6) should keep the trapped carriers for milliards of years. Only carriers in the two traps producing the TL band below 200 °C are able to escape them within hours, which indeed takes place as the material shows visible afterglow for some time. After a few hours in darkness, this component is no longer seen in the TL glow curve, as will be presented later.

TL glow curves of Lu_2O_3:0.05%Pr,0.1%Hf ceramics as a function of irradiation time with X-Rays are presented in Figure 4a. The band positions (maxima) occur perfectly at the same temperatures, which is one of the criteria proving the first-order kinetics.[27] This result further supports the conclusions from the glow curve deconvolution presented above. Independently on the irradiation time (the dose) all the taps contribute to the thermoluminescence. However, the least intense structure around 135 °C saturates within first few minutes of the irradiation, while the two others located at higher temperatures seem to follow the linear increase of intensity (in log-log scale) at least within the first 60 minutes of irradiation, see Figure 4b.

Figure 5 compares the TL glow curves of the Lu_2O_3:0.05%Pr,0.1%Hf material recorded with different delay time after UV irradiation. It is clear that 4 hours is enough to lose all the energy stored in traps producing the TL signal around 135 °C, as this component completely vanishes from the glow curve after such a time. This is consistent with the trap lifetimes given in Table 1. As expected, intensities of the higher-temperature TL components are hardly affected even after having the irradiated specimen for 17 days in darkness. Yet, a small decrease of the signal around 250 °C without any changes about 340 °C is seen. However, 9 months delay gives TL signal whose intensity comprised in both the high-temperature components is reduced by almost 30%. This loss is higher than predicted by the calculated trap lifetimes given in Table 1. Hence, even energy from the deep traps can partially leak out of them at RT within a few months though the Arrhenius dependence predicted much better stability. It is not a trivial effect and its grounds are not fully understandable at present. A possible explanation could be a slow cascade detrapping (CD). Such a mechanism was reported for TL bands with high frequency factors combined with high activation energies,[28] similarly to what we observe. Yet, at this stage, it remains a presumption and not a conclusive statement. Nevertheless, the stability of the TL signal in time is very good and may make the Lu_2O_3:Pr,Hf composition an interesting material for high energy particles dosimetry in some circumstances.

Figure 6a compares TL glow curves recorded using a specific procedure: first the sample was X-Rayed at RT then its temperature was raised to a defined value (given in Figure 6a) and immediately cooled to RT. Afterwards, a TL glow curve was recorded. This set of experiments gave an elegant, clear confirmation of the structure of traps we received from deconvolution of the glow curve given in Figure 3. First of all, it appears clear that the TL band peaking around 250 °C is composed of two components among which the higher-temperature one was nicely

exposed by TL glow curve recorded on the material shortly preheated up to 215 °C as well as 225 °C. Its position in Figure 6a coincides with the component #4 seen in Figure 3 and Table 1. What is more, the TL curves recorded after preheating of the sample at the temperatures in the range of 245-315 °C clearly shows that the intensity of the TL band peaking around 340 °C gets continuously reduced as the preheating temperature gets higher and that this effect is much stronger at the low-temperature side of this TL band. Such a behavior is also consistent with the findings seen in Figure 3, where the highest-temperature TL band was found to be a superposition of two strongly overlapping components, resulting from traps with similar parameters (Table 1). Experiments whose results are given in Figure 6b support the above conclusions. This figure gives a set of glow curves recorded when the sample after being X-Rayed was additionally exposed to 980 nm, 780 nm or 400 nm radiation. The 980 nm stimulation (red line) removes the low temperature components (#1-3) from the TL glow curve leaving basically unaffected the constituents #4-6 (see also Figure 3 and Table 1). The band located around 135 °C disappears completely together with a significant portion of the main TL constituent around 250 °C. Note, that this is the low temperature fraction of the main TL band (~250 °C) which disappeared upon the 980 nm radiation. Consequently, the trap #4 was basically unaffected. Hence, the 980 nm (~1.26 eV) radiation is able to kick off the carriers from traps #1-3 without touching carriers in traps #4-6. Stimulation with 780 nm (~1.6 eV) radiation bleaches, though only partially (hence: with difficulty), also the trap #4. Clearly, such radiation carries energy which is hardly enough to reach the depth of the trap #4. This is quite reasonable, as this trap was found to have depth of about 1.7 eV (Table 1), which is slightly more than the 780 nm light carries. Yet, such conclusions should be taken with care as the mechanisms of both stimulations are so different that such elementary analogies can easily be oversimplified. Yet,

the carriers from traps giving TL around 340 °C (#5 and #6) are not at all affected upon treatment with 780 nm radiation. This is the continuous irradiation with light of about ~400 nm wavelength (~3 eV) which fully bleaches all the traps, as is seen in Figure 6b. Whichever is the stimulation, the emission comes exclusively from Pr^{3+} ions and appears in the red, as was presented in Figure 2. It is quiet specific situation as usually the stimulating radiation is of lower energy than the emitted one. Typically, the reading is performed by radiation whose energy is lower than luminescence caused by it.

Figure 7a shows changes in absorption of the ceramics induced by various irradiations, exactly the same as indicated in Figure 6b. Clearly, X-Ray irradiation suppressed the absorption in the short-UV region, where Pr^{3+} f-d bands are present. This effect is mirrored by an appearance of a broad band absorption in the ~370-650 nm region. After subsequent stimulation with 980 nm and even more with 780 nm radiation the changes were partially reversed, especially in the long wavelength region (~450-650 nm). However, only the treatment with 400 nm radiation (as well as heating up to about 350 °C, which result is not presented in Figure 7a) restored the absorption of the raw, untreated specimen. Upon such treatment both the X-Ray induced absorption band around 340-650 nm disappeared and the Pr^{3+} f$\rightarrow$d absorption in deep-UV regained its original intensity of the fresh ceramics.

The 340-650 nm absorption band seems to comprise of at least two components, as the IR photons (especially the 780 nm) reduced its intensity in the long-wavelength region rather, while the absorption around 340-420 nm was barely affected. Part of the changes in absorption due to the various treatments were seen by eye - the X-Rayed specimen got rosy in color and the subsequent 400 nm irradiation turned it back almost white. The rosy color got deeper when the sample was X-Rayed for longer time.

Measurements of excitation spectra of the raw and irradiated sample proved that the near-UV-Vis absorption induced by X-Rays is indeed a doublet. The results are presented in Figure 7b. After irradiation with X-Rays a new excitation band covering the ~340-430 nm range of wavelengths is evident. It is yet much narrower than the extrinsic absorption seen in Figure 7a. This is evidence that the X-Ray induced absorption results from (at least) two different entities. In the inset of Figure 7b we show how the Pr^{3+} luminescence decays upon continuous stimulation with 400 nm radiation. The emission could be easily recorded for an hour or so and its decay trace could be fitted with eq 3 using the parameter n=0.8. Yet, it has no physical meaning here as its value depends not only on the mechanism of the luminescence but also on the (uncontrolled, though constant during the experiment) intensity of the stimulating light. In the X-rayed specimen the excitation spectrum in the deep UV got significant enhancement. This is surprising at first, as absorption in this region (Figure 7a) was significantly reduced at the same time. Yet, such a contradictory behavior is reasonable, as through irradiation with X-Rays the traps are being filled and during the measurement of the excitation spectrum the electrons excited to the 5d levels cannot escape the mother ions having no empty reservoir available. Consequently, excitation into UV gets enhancement.

The systematic changes observed in TL presented in Figure 6a,b and mirrored with the variations in absorption presented in Figure 7a allows to relate them. Thus, freeing the traps #1-3 (980 nm) does not affect absorption below 600 nm. Yet, even partial emptying of the trap #4 (upon 780 nm stimulation) evidently reduces the extrinsic broad absorption spreading around 475 nm with a slight enhancement in the range of Pr^{3+} f→d transitions at the same time. This radiation also only slightly reduces the extrinsic absorption around 370 nm.

Clearly, (most of) the reduced absorption of Pr^{3+} ion in deep UV is connected with the two deepest traps giving TL around 340 °C as only depleting them completely restores the intensity of the Pr^{3+} f→d absorption to the level observed in the raw, untreated specimen. This is an important sign that in the doubly doped ceramics Pr^{3+} actively participates in energy storing, and not only in producing emission. Yet, only the deepest traps seem to be *directly* connected with this dopant.

The changes in absorption induced by X-Rays and the rosy body color of irradiated ceramics could be connected with the partial Pr^{3+}→Pr^{4+} oxidation. The O^{2-}→Pr^{4+} charge transfer transition indeed should be located in the near-UV or Vis part of spectrum. This would also explain the reduced absorption in the region of the f→d transitions of the Pr^{3+} (below about 330 nm). Yet, the broad band in near-UV and Vis may easily result from trapped electrons in O-vacancies or at the Hf^{4+} codopant. We already mentioned that the broad X-Ray induced absorption comprises two components – this was evident from comparison of absorption and excitation spectra given in Figure 7a,b. Hence, it appears reasonable that two different entities give rise to the broad band appearing after exposure to X-Rays and connected with energy storing in Lu_2O_3:Pr,Hf.

Figure 8 presents isothermal decay traces of Lu_2O_3:0.05%Pr,0.1%Hf ceramics obtained at seven different temperatures in the range of 150 °C - 210 °C after irradiation with X-Rays. The experimental data were fitted with eq 3:

$$I(t) = I_0 \times (1 + \gamma t)^{-n}, \quad (3)$$

where $\gamma = N/(a n_{t0})$, N corresponds to the density of trapping centers, n_{t0} is the population of holes in the trapping centers at time $t = 0$, and a describes the detrapping rate.[29] The fitting parameter n increases from around 2 to about 4 (exact numbers a given in Figure 8) when the sample temperature increases from 150 °C to 210 °C. This change indicates that the retrapping

becomes continuously less efficient with rising temperature.[30] This is exactly what one may expect when temperature of the sample gets higher.

In Figure 9a TL glow curves of X-Rayed Lu_2O_3:0.05%Pr,0.1%Hf ceramics during heating with different rates from 1 to 8 °C/s are presented. No spectacular changes in the glow curves structure has been observed for different heating rates and always three main components were observed. The peak positions move towards higher temperatures with increasing heating rate, which is a typical effect. [9,31,32] Figure 9b shows that the variation of the peak heights for the three main bands as a function of the heating rate is insignificant, within an experiment precision. The correction for the thermal quenching (see Figure 1) was applied for these results.

DISCUSSION

The results given in Figure 1 are straightforward: efficient energy storing in Lu_2O_3 requires *both* Pr and Hf to be present in the Lu_2O_3 host. Hence, the energy storing is a *co-operative* effect of both dopants. Introduction of Hf has at least two important consequences. Not only do we get $Hf^{\bullet}_{Lu}$ defects with positive net charge, which thus may attract electrons, but this charge has to be compensated to assure the host electrostatic neutrality. An apparent pathway of achieving it is incorporation of interstitial oxygen, O''_i, whose doubly negative net charge would balance two $Hf^{\bullet}_{Lu}$ sites. Let us note, that incorporation of O''_i would be facilitated by the lutetia host structure, as in this fluoride-type lattice two empty O-sites in the nearest coordination sphere of each metal cation are inherently present. Accordingly, we may reasonably assume that in the synthesized materials the following defect sites capable of participating in the TL process are present: Pr^{X}_{Lu}, $Hf^{\bullet}_{Lu}$, and O''_i.

Pr_{Lu}^{X} is at first the emitter, hence the stored energy has to get to it somehow. Yet, it can also be an $h^{\bullet}$-trapping center, as it may be capable of turning into a stable Pr^{4+} state, or $[Pr^{3+}\text{-}h^{\bullet}]$ entity, similarly to Tb^{3+} activated persistent phosphors reported earlier [12,33]. Yet, as Figure 1 shows, in the Pr singly doped composition the energy is hardly stored giving rise to only inefficient TL around 340 °C. This might suggest that Pr_{Lu}^{X} is not an efficient trap. However, since $Hf_{Lu}^{\bullet}$ is a perfect (potential) e'-trapping center, as its positive net charge necessarily attracts the electron excited to the conduction band of the host, this process may also facilitate trapping hole in Pr_{Lu}^{X} stabilizing Pr^{4+} or $[Pr^{3+}\text{-}h^{\bullet}]$ state. On the other hand, interstitial oxygen, $O_i^{''}$, whose presence, as was discussed, is justified by the introduction of Hf, can easily serve as an $h^{\bullet}$-trapping site too, due to its negative net charge. Hence, we could write the following equations to show processes through which the energy is being stored in the Lu_2O_3:Pr,Hf ceramics:

$$Hf_{Lu}^{\bullet} + e' \rightarrow Hf_{Lu}^{\times} \quad (4)$$

$$O_i'' + h^{\bullet} \rightarrow O_i' \quad (5)$$

$$Pr_{Lu}^{\times} + h^{\bullet} \rightarrow Pr_{Lu}^{\bullet} \quad (6)$$

While the process described with eq 5 is formally possible, if hole was trapped in such a way this would leave the Pr^{3+} absorption after irradiation basically unaffected. Yet, the measurements proved a very significant reduction of the f→d Pr^{3+} absorption for X-rayed sample (Figure 7a). Hence, trapping the hole at Pr^{3+} site appears more confident. On the other hand, one may argue that both (5) and (6) occurs. Presently, we are not in the position to definitely resolve this dilemma.

From the published data[34] and the Dorenbos' model[5] we calculated the position of the Pr^{3+} electronic levels in Lu_2O_3, whose band gap energy is about 5.6 eV at RT[35]. This allowed us to develop a scheme of the electronic states of entities actively participating in the energy storing and in the TL process of Lu_2O_3:Pr,Hf ceramics. This is presented in Scheme 1. The 5d levels of

Pr^{3+} are immersed within the conduction band, which explains why not only X-Rays but also the short UV radiation through efficient f→d absorption fills the traps. Simply, the electron excited to 5d states of Pr^{3+} couples with the states of the host conduction band and thus it can escape its mother ion, diffuse for some distance to get trapped in a defect, presumably the $Hf^{\bullet}_{Lu}$ site, as we already stated. Analogous trapping occurs upon irradiation with X-Rays.

The TL at the highest temperature, around 340 °C should then result from the hole trapped at Pr^{X}_{Lu} forming $[Pr^{3+}\text{-}h^{\bullet}]/Pr^{\bullet}_{Lu}$ entity. Formation of $Pr^{\bullet}_{Lu}$ was already postulated by changes in the deep UV part of absorption spectra induced by X-Rays (Figure 7a) which indicated reduced population of Pr^{3+} ions after irradiation with X-Rays. Yet, contribution from the $O_i^{''}$ to this TL band is not excluded.

We assign the TL around 250 °C to the energy stored in $Hf^{\bullet}_{Lu}$. The 250 °C TL was not present even as a trace until Hf was added, see Figure 1. This band was showed to comprise two components (Figure 7). Temporarily, we think that they may reflect the presence of two metal sites, C_2 and C_{3i}, in the host material.

Now, let us deal with the low intensity TL around 135 °C. Such a TL band, but much more intense, was already reported for an efficient persistent phosphor, Lu_2O_3:Tb,Ca,[12,13] prepared in reducing atmosphere. Very similar situation to Lu_2O_3:Tb,Ca we observe in Lu_2O_3:Pr,Ca, which was not yet published. It was convincingly argued in[13] that the 135 °C TL resulted from O-vacancies abundant in Lu_2O_3:Tb,Ca due to the reducing atmosphere of preparation and necessity to compensate negative net charge of Ca^{2+} which replaced Lu^{3+}. In Lu_2O_3:Pr,Hf the TL around 135 °C is a minor constituent of the whole TL glow curve as in this case there are not favorable conditions to create O-vacancies. Yet, their existence as low population defects can be justified by the high temperature of preparation of the investigated ceramics. At such conditions,

formation of Schottky defects is unavoidable and thus presence of some O-vacancies is validated. Summarizing, the TL of Lu_2O_3:Pr,Hf ceramics above 200 °C is due to the Pr and Hf co-doping, while the one below 200 °C is a consequence of formation of vacant oxygen sites due to the high temperature of the ceramics' preparation. In fact the TL below 200 °C, responsible for some small RT afterglow, is a drawback of the Lu_2O_3:Pr,Hf storage phosphor. Yet, till now we were not able to get rid of it by means of technological tricks.

All the high temperature components of the TL glow curve (>200 °C) were found to have the frequency factors exceeding the Debye frequency (~10^{13} s^{-1}) by 3-4 orders of magnitude, see Table 1. Such high rates suggests that the mechanism of the thermally stimulated luminescence has mixed character and it is probable that the carriers get to the emitting ion not only by being excited to the conduction/valence band but also, simultaneously, by means of another channel. On the other hand, since the TL glow curve has several overlapping glow peaks the parameters derived from fitting may be burden with significant inaccuracy. As noted by Bos[27] the simple model describing the kinetics of the TL phenomenon fails in the case of overlapping TL components. Consequently, deconvolution of complex TL glow curves gives trap parameters whose values and physical meaning are doubtful. And we should keep it in mind concluding on TL properties of Lu_2O_3:Pr,Hf ceramics.

The $Hf^{\bullet}_{Lu}$ and $O_i^{''}$ defects, owing to their net charges, can be expected to cluster forming spatially linked energy trapping complex sites. Since Hf^{4+} is smaller and Pr^{3+} is larger than Lu^{3+}, we may further expect that even Pr^{X}_{Lu} may tend to aggregate with $Hf^{\bullet}_{Lu}$ and $O_i^{''}$ defects. This reasoning gets important support from the fact that high-temperature preparation significantly enhances TL efficiency (detailed results how fabrication temperature affects the TL properties were not presented in this paper).

It was indicated in[28] that the temptation to treat the traps uniformly distributed within the host is often unjustified. Traps (defects) may be forced to cluster as this may be thermodynamically advantageous. From what was said above we have good reasons to postulate that such an effect plays an important role in Lu_2O_3:Pr,Hf storage phosphor and point defects form the [$Hf^{\bullet}_{Lu}$-Pr^{X}_{Lu}-$O_i^{''}$] spatially correlated structures. And only then, when the distance between the various taps is reduced can efficient TL be generated.

Furthermore, the spatial correlation could also be blamed for the observed energy sink from the deep traps (Figure 5) seen after a few months, while from the traps parameters their stability should be higher (Table 1). We claim that this is the spatial correlation of the point defects which allows for their communication and energy exchange leading to the observed fading. Note that the $^1D_2$ emitting level of Pr^{3+} and the $Hf^{\bullet}_{Lu}$ trap state energetically coincide (Scheme 1), which such energy diffusion may make only more probable. Thus all the results can be logically combined into a consistent picture explaining the properties of the Lu_2O_3:Pr,Hf storage phosphor ceramics.

CONCLUSIONS

In this paper we report on spectroscopic properties of the Lu_2O_3:Pr,Hf sintered ceramic storage phosphors and discuss the mechanisms standing behind the observed processes. The whole variety of experimental data collected measuring thermoluminescence, optically stimulated luminescence, fading, isothermal decay traces, photoluminescence and excitation spectra, luminescence decay times as well as data from analytical deconvolution of the glow curves gave consistent picture as to the physics standing behind the thermoluminescence. The glow curve deconvolution gave as much as six, partly overlapping components forming three bands peaking

around 130 °C, 250 °C and 340 °C. It was found that the last two, being the main TL constituents, result from Hf(IV) replacing Lu(III) in the host (250 °C) and the Pr^{3+} activator itself, maybe with some contribution from interstitial oxygen (340 °C). Trap depths were found to cover the 0.8-2.1 eV range of energies. The TL process was found to follow the first-order kinetics. It was showed that bleaching of the traps giving rise to the TL at lower temperatures (traps #1-3) is possible without affecting the energy stored in the other traps. Furthermore, energy from the trap #4 could also be freed without loss of carriers entrapped in traps #5 and #6. This could be attained either by controlled thermal stimulation or with infrared photons whose energy was properly tuned. The stored energy could be freed totally by heating the materials up to about 450 °C or with ~400 nm radiation. Changes observed in absorption and excitation spectra were harmonized with the variations in the course of the glow curve and altogether a consistent picture the observed spectroscopic processes was obtained. Agglomeration of defects due to the high temperature fabrication process was postulated to be beneficial for TL efficacy, e.g. for the amount of energy possible to freeze in the Lu_2O_3:Pr,Hf ceramics. Fading was found to reach only about 30% within the first nine months. Such a good long term stability of the thermoluminescence signal and high efficiency of absorption of ionizing radiation of the lutetia host may make the Lu_2O_3:Pr,Hf composition an interesting material for high energy gamma particles dosimetry.

FIGURES

Figure 1. TL glow curves of undoped Lu_2O_3, singly doped Lu_2O_3:0.05%Pr, and Lu_2O_3:0.1%Hf and doubly doped Lu_2O_3:0.05%Pr,0.1%Hf ceramics measured immediately after irradiation with X-Rays. The blue curve with dots gives a temperature dependence of the decay time of Pr^{3+} luminescence.

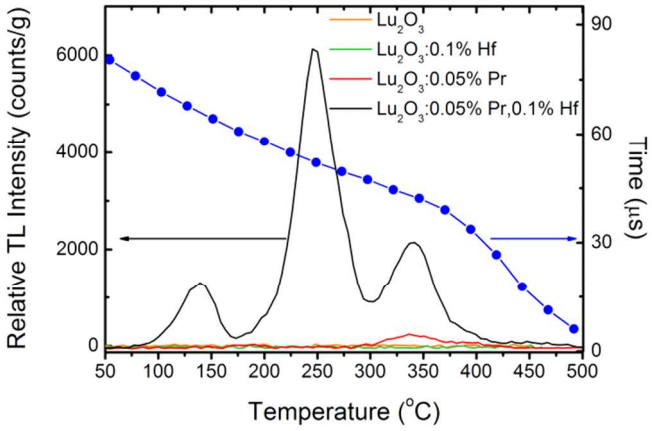

Figure 2. Room temperature excitation spectra of 610 nm and 631.5 nm emissions (left), photoluminescence spectrum under 275 nm excitation and thermoluminescent emission spectrum of Lu_2O_3:0.05%Pr,0.1%Hf ceramics recorded at 250 °C (right).

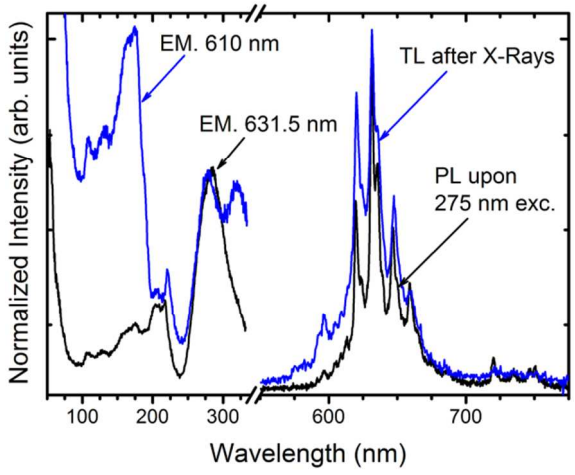

Figure 3. TL glow curve of Lu_2O_3:0.05%Pr,0.1%Hf ceramics recorded after irradiation with X-Rays for 5 minutes (solid line). Deconvolution of the experimental curve using the first-order kinetics gave six components presented with dotted lines. Constituent #2 has negligible intensity. See also Table 1.

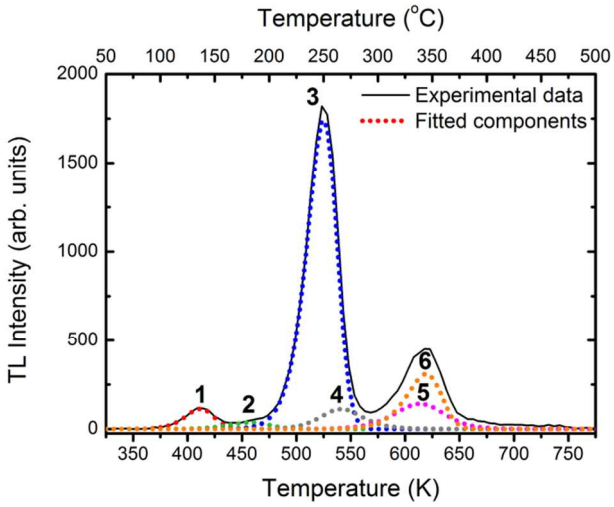

Figure 4. Influence of irradiation time with X-Rays on the thermoluminescence glow curves of Lu_2O_3:0.05%Pr,0.1%Hf ceramics (a), and integrated TL intensities of the three bands (b). The solid lines introduced just to guide the eye.

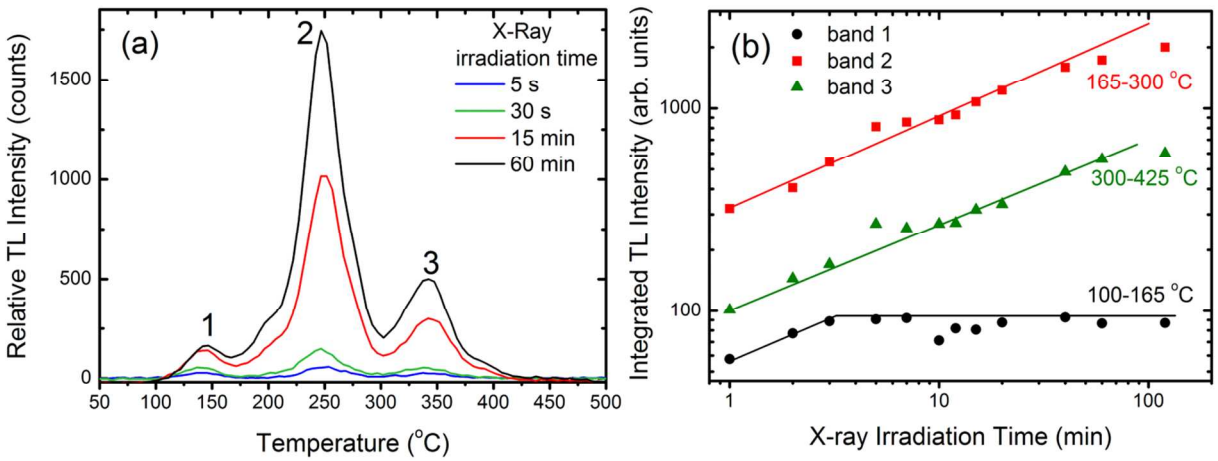

Figure 5. TL glow curves of the Lu_2O_3:0.05%Pr,0.1%Hf ceramics measured following different delay time (indicated in the figure) after its exposure into 254 nm UV radiation for 15 minutes. The sample was kept at RT all the time.

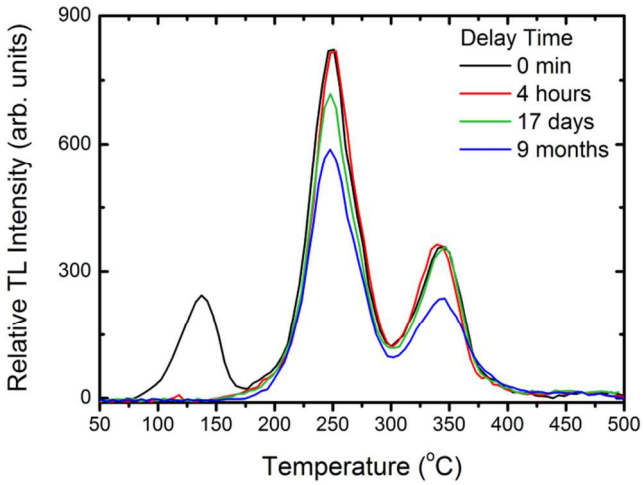

Figure 6. TL glow curves of Lu_2O_3:0.05%Pr,0.1%Hf ceramics measured shortly after X-Ray irradiation and after subsequent preheating to different temperatures from 160 °C to 315 °C (a). TL glow curves measured shortly after X-Ray irradiation and after subsequent stimulation with 980 nm, 780 nm, 400 nm diode lasers for 30 minutes (b).

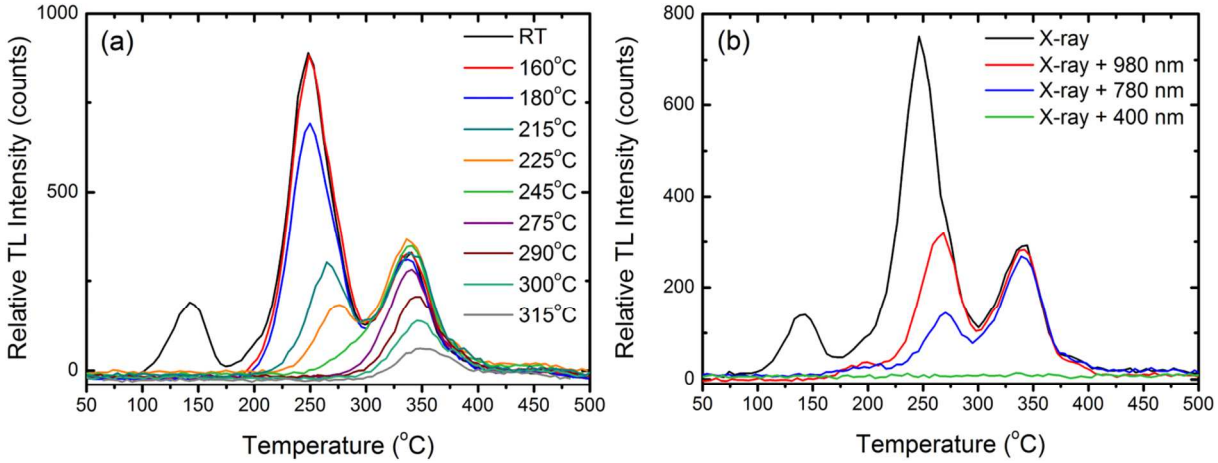

Figure 7. Absorption spectra of Lu_2O_3:0.05%Pr,0.1%Hf raw ceramics and after X-Ray irradiation and additional stimulation with 980 nm, 780 nm, 400 nm diode lasers for 30 minutes (a). Excitation spectra of 632 nm emission of raw sample and after X-Ray irradiation followed by additional 400 nm stimulation for 15 minutes (b). Insert in (b): Logarithmic dependence of luminescence intensity vs. time recorded during 400 nm continuous stimulation following the X-Ray irradiation.

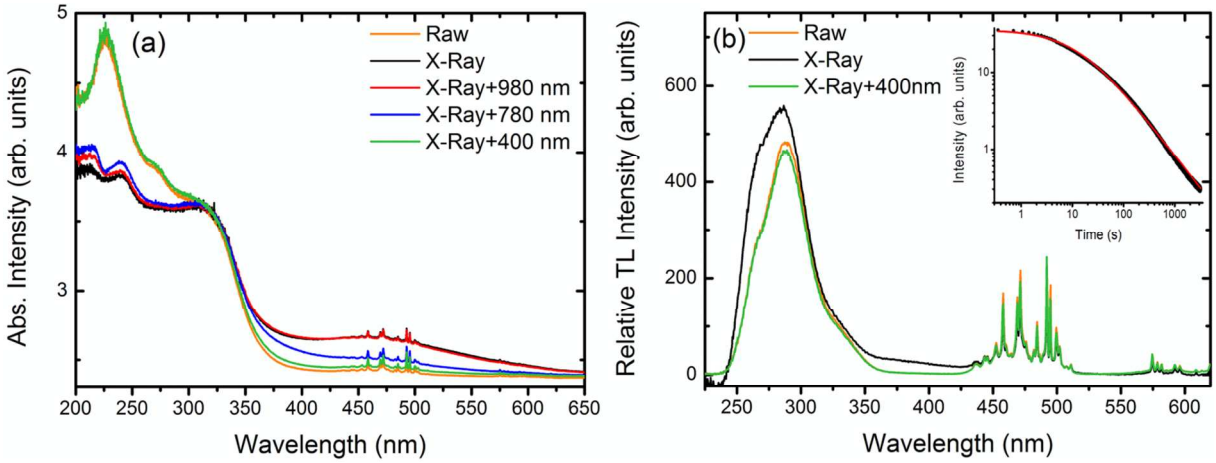

Figure 8. The isothermal phosphorescence decay traces of Lu_2O_3:0.05%Pr,0.1%Hf ceramics recorded at seven different temperatures from 150 °C to 210 °C after 5 minutes X-Ray irradiation. Solid lines results from fits with eq 3.

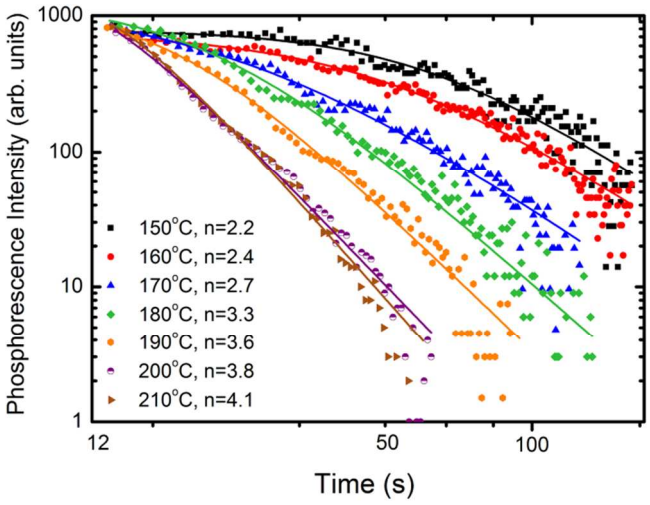

Figure 9. Normalized to the same height TL glow curves of Lu_2O_3:0.05%Pr,0.1%Hf ceramics measured with different heating rate of 1, 2, 5, 8 °C/s after irradiation with X-Rays (a). Variation of the intensities (height/β) of the three main bands of glow curves as a function of the heating rate (b).

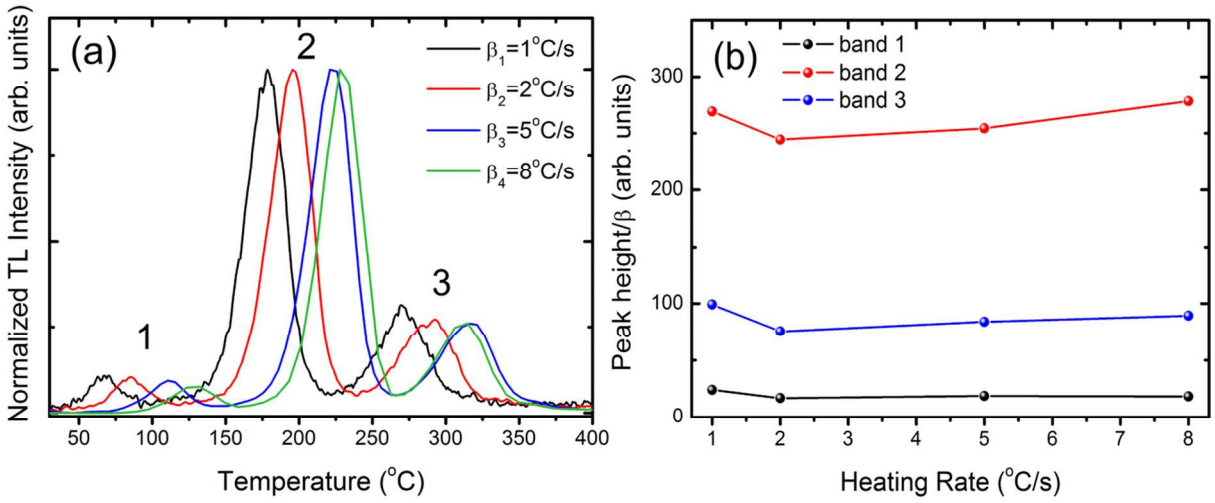

SCHEMES

Scheme 1. Scheme of the electronic states involved into the energy storing and connected with $Pr^{X}_{Lu}/O_i^{''}$, $Hf^{\bullet}_{Lu}$, $V_O^{\bullet\bullet}$ defects, related to the Pr^{3+} levels and the host band structure.

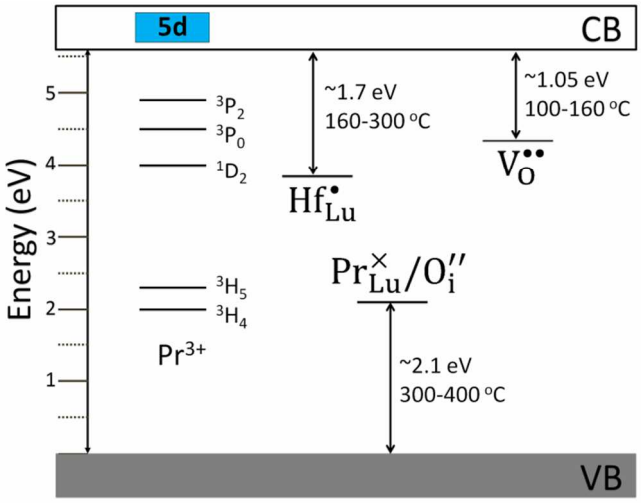

TABLES

Table 1. Table 1. Parameters of the traps derived by the deconvolution of the measured TL glow curve of Lu_2O_3:0.05%Pr,0.1%Hf ceramics obtained using first-order kinetics approach.

Trap No.	T (°C)	E (eV)	s (s^{-1})	τ (h)
1	137	1.14	1×10^{14}	113

2	181	0.83	3×10^{9}	17.5
3	250	1.69	4×10^{16}	8.2×10^{8}
4	270	1.71	2×10^{16}	3.6×10^{9}
5	335	2.11	3×10^{17}	1.8×10^{15}
6	345	2.05	5×10^{16}	1×10^{15}

Displayed equations

$$I\,(t) = -\frac{dn}{dt} = sn\exp\left(-\frac{E}{kT}\right), \quad (1)$$

$$\tau = s^{-1}\exp(\frac{E}{kT}) \quad (2)$$

$$I\,(t) = I_0 \times (1+\gamma t)^{-n}, \quad (3)$$

$$\mathrm{Hf}_{\mathrm{Lu}}^{\bullet} + \mathrm{e}' \rightarrow \mathrm{Hf}_{\mathrm{Lu}}^{\times} \quad (4)$$

$$\mathrm{O}_{\mathrm{i}}'' + \mathrm{h}^{\bullet} \rightarrow \mathrm{O}_{\mathrm{i}}' \quad (5)$$

$$\mathrm{Pr}_{\mathrm{Lu}}^{\times} + \mathrm{h}^{\bullet} \rightarrow \mathrm{Pr}_{\mathrm{Lu}}^{\bullet} \quad (6)$$

AUTHOR INFORMATION

Corresponding Author

*eugeniusz.zych@chem.uni.wroc.pl

Tel. +48 71 3757248

Fax. +48 71 3282348

Funding Sources

The research was supported by Wroclaw Research Centre EIT+ within the project "The Application of Nanotechnology in Advanced Materials" - NanoMat (POIG.01.01.02-02-002/08) financed by the European Regional Development Fund (Innovative Economy Operational Program 1.1.2). We also acknowledge partial support by DESY Hasylab Grant # II-20090289 EC.

ACKNOWLEDGMENT

The authors are indebted to Professor Arkadiusz Mandowski from Jan Dlugosz Academy in Czestochowa, Poland for stimulating discussions and suggestions.

REFERENCES

[1] McKeever, S. W. S. *Thermoluminescence of Solids*, Cambridge University Press, Cambridge, U.K., **1985**.

[2] Chen, R.; McKeever, S. W. S. *Theory of Thermoluminescence and Related Phenomena*, World Scientific, Singapore, **1997**.

[3] Furreta, C. *Handbook of Thermoluminescence*, World Scientific, Singapore, **2003**.

[4] Hölsä, J.; Laamanen, T.; Lastusaari, M.; Malkamäki, M.; Novák, P. *J. Lumin*. **2009**, 129, 1606.

[5] Dorenbos, P.; Bos, A. J. J. *Radiat. Meas.* **2008**, 43, 139.

[6] Bos, A. J. J.; Dorenbos, P.; Bessière, A.; Viana, B. *Radiat. Meas.* **2008**, 43, 222.

[7] Lecointre, A.; Bessière, A.; Bos, A. J. J.; Dorenbos, P.; Viana, B.; Jacquart, S. *J. Phys. Chem. C* **2011**, 115, 4217.

[8] Dorenbos, P.; Bos, A. J. J.; Poolton, N. R. J. *Opt. Mater.* **2011**, 33, 1019.

[9] Bos, A. J. J.; Dorenbos, P.; Bessière, A.; Lecointre, A.; Bedu, M.; Bettinelli, M.; Piccinelli, F. *Radiat. Meas.* **2011** doi:10.1016/j.radmeas.2011.04.021.

[10] Leverenz, H.W. *An Introduction to Luminescence of Solids*, John Wiley and Sons, New York, USA, **1950**.

[11] Daunay, J.; Daunay J.; Batailler, G. *J. Lumin*. **1973**, 6, 44.

[12] Trojan-Piegza, J.; Niittykoski, J.; Hölsä, J.; Zych, E. *Chem. Mater.* **2008**, 20, 2252.

[13] Trojan-Piegza, J.; Zych, E.; Hölsä, J.; Niittykoski, J. *J. Phys. Chem. C* **2009**, 113, 20493.

[14] Kulesza, D.; Trojan-Piegza, J.; Zych, E. *Radiat. Meas.* **2010**, 45, 490.

[15] Kulesza, D.; Wiatrowska, A.; Trojan-Piegza, J.; Felbeck, T.; Geduhn, R.; Motzek, P.; Zych, E.; Kynast, U. *J. Lumin*. **2013**, 133, 51.

[16] Zych, E.; Wiatrowska, A. *Luminescent material as well as a method of obtaining it,* PTC/PL2012/050002.

[17] Pechini, M. P. *Method of preparing lead and alkaline earth titanates and niobates and coating method using the same to form a capacitor*, U. S. Patent 3,330,697, **1967**.

[18] Puchalska, M.; Bilski, P. *Radiat. Meas.* **2006**, 41, 659.

[19] Kröger, F. A.; Vink. H. H. In *Solid State Phys.*; Seitz, F; Turnbull, D. Eds.; Academic Press: San Diego, CA **1956**; Vol. 3, p 273.

[20] http://old.iupac.org/publications/books/rbook/Red_Book_2005.pdf.

[21] FindIt Database (ICSD#40471).

[22] Trojan-Piegza, J.; Zych, E. *J. Alloy. Compd.* **2004**, 380, 118.

[23] Wang, Z.; Zhang, W.; Lin, L.; You, B.; Fu, Y.; Yin, M. *Opt. Mater*. **2008**, 30, 1484.

[24] Galceran, M.; Pujol, M.C.; Aguiló, M.; Díaz, F. *Mater. Sci. Eng. B* **2008**, 146, 7.

[25] De Mello Donegá, C.; Meijerink, A.; Blasse, G.; *J. Phys. Chem. Solids* **1995**, 56, 673.

[26] Zych, E.; Wawrzyniak, M.; Kossek, A.; Trojan-Piegza, J.; Kępiński, L. *J. Alloy. Compd.* **2008**, 451, 591.

[27] Bos, A. J. J. *Radiat. Meas.* **2007**, 41, S45.

[28] Mandowski, A. *Radiat. Prot. Dosim.* **2006**, 119(1-4), 23.

[29] Nakazava, E. In *Phosphor Handbook*; Shionoya, S.; Yen, W. M. Eds.; CRC Press, Boca Raton, **1999**, p 85.

[30] Jia, D.; Zhu, J.; Wu, B. *J. Lumin*. **2000**, 91, 59.

[31] Anishia, S. R.; Jose, M. T.; Annalakshmi, O.; Ramasamy, V. *J. Lumin*. **2011**, 131, 2492.

[32] Krumpel, A. H.; Van der Kolk, E.; Zeelenberg, D.; Bos, A. J. J.; Krämer, K. W.; Dorenbos, P. *J. Appl. Phys.* **2008**, 104, 073505.

[33] Hosono, H.; Kinoshita, T.; Kawazoe, H.; Yamazaki, M.; Yamamoto, Y.; Sawanobori, N. *J. Phys.: Condens. Matter* **1998**, 10, 9541.

[34] Yen, W. *J. Lumin*. **1999**, 83-84, 399.

[35] Prokofiev, A. V.; Shelykh, A. I.; Melekh, B. T. *J. Alloy. Compd.* **1996**, 242, 41.

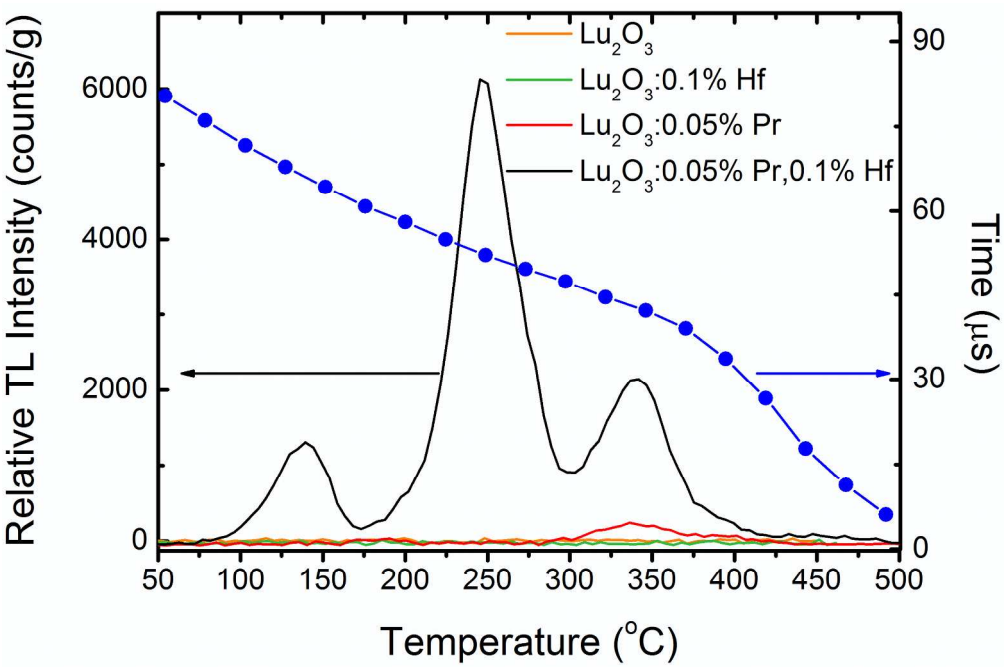

1069x708mm (72 x 72 DPI)

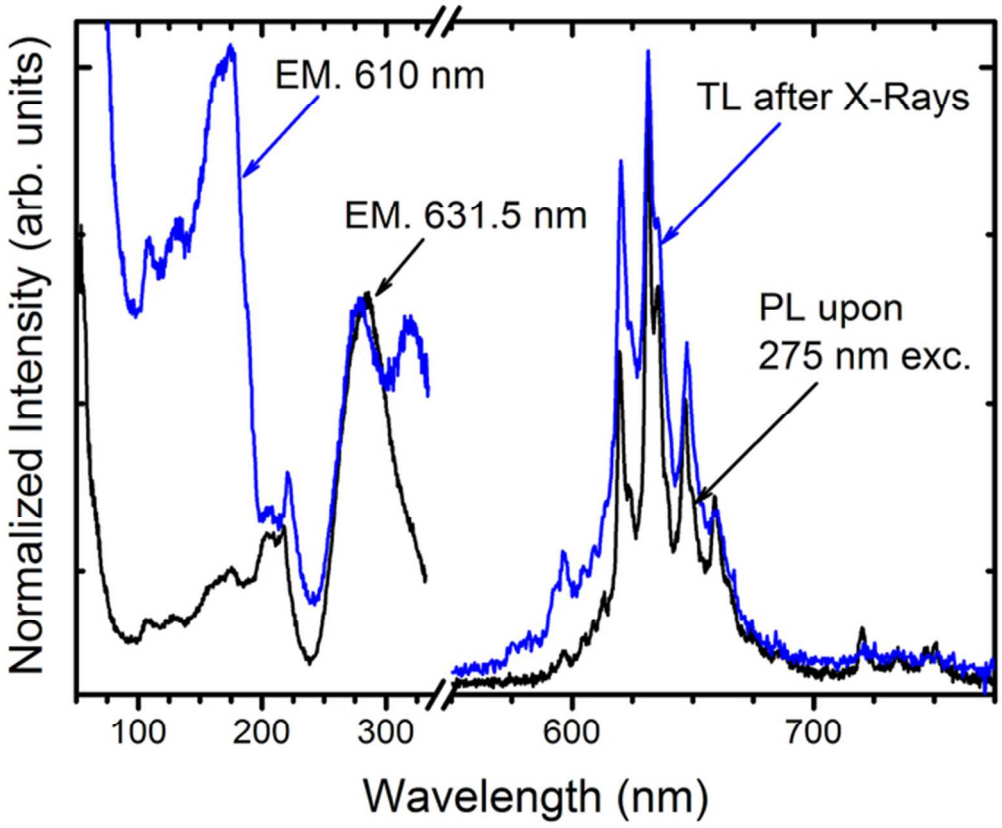

57x47mm (300 x 300 DPI)

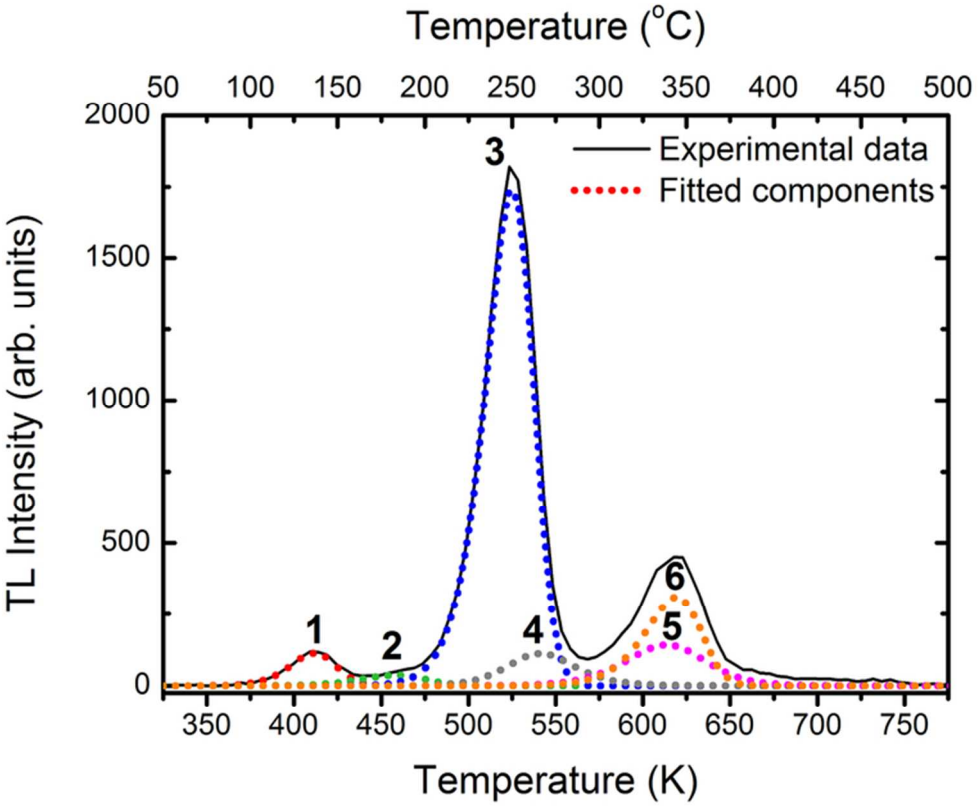

66x52mm (300 x 300 DPI)

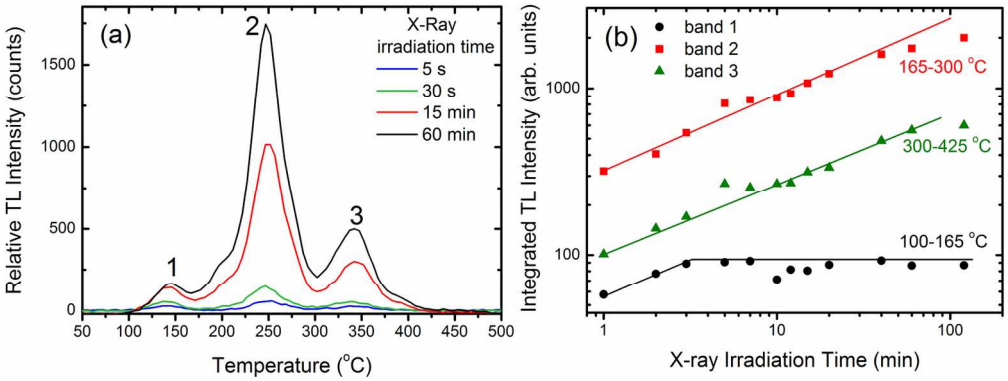

160x60mm (300 x 300 DPI)

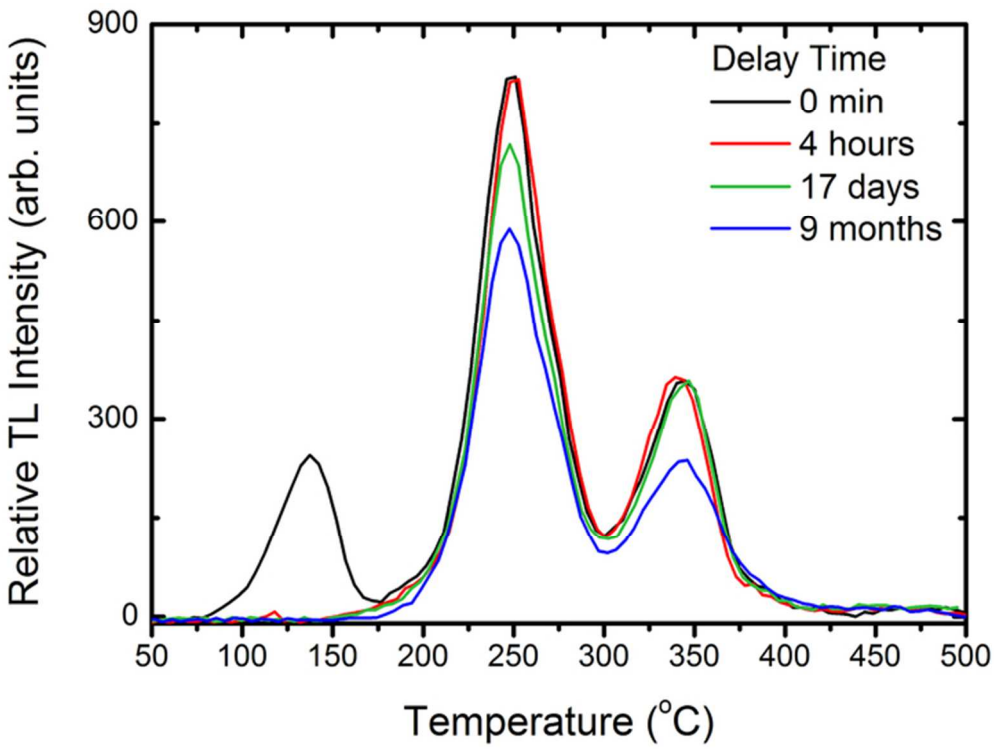

61x45mm (300 x 300 DPI)

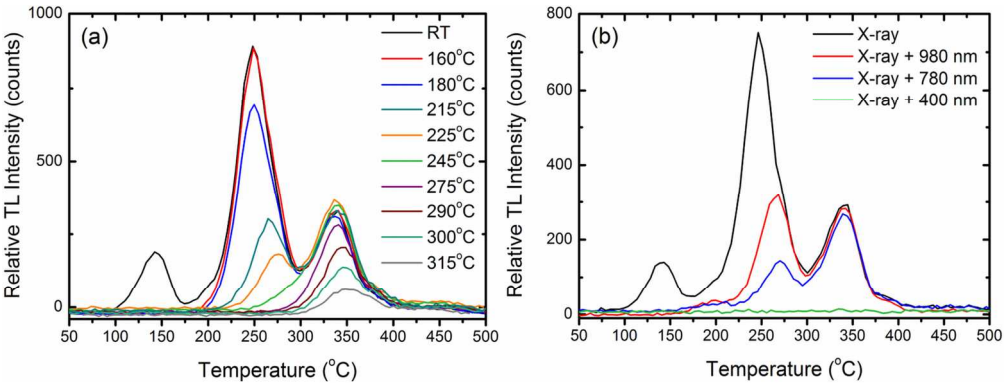

160x60mm (300 x 300 DPI)

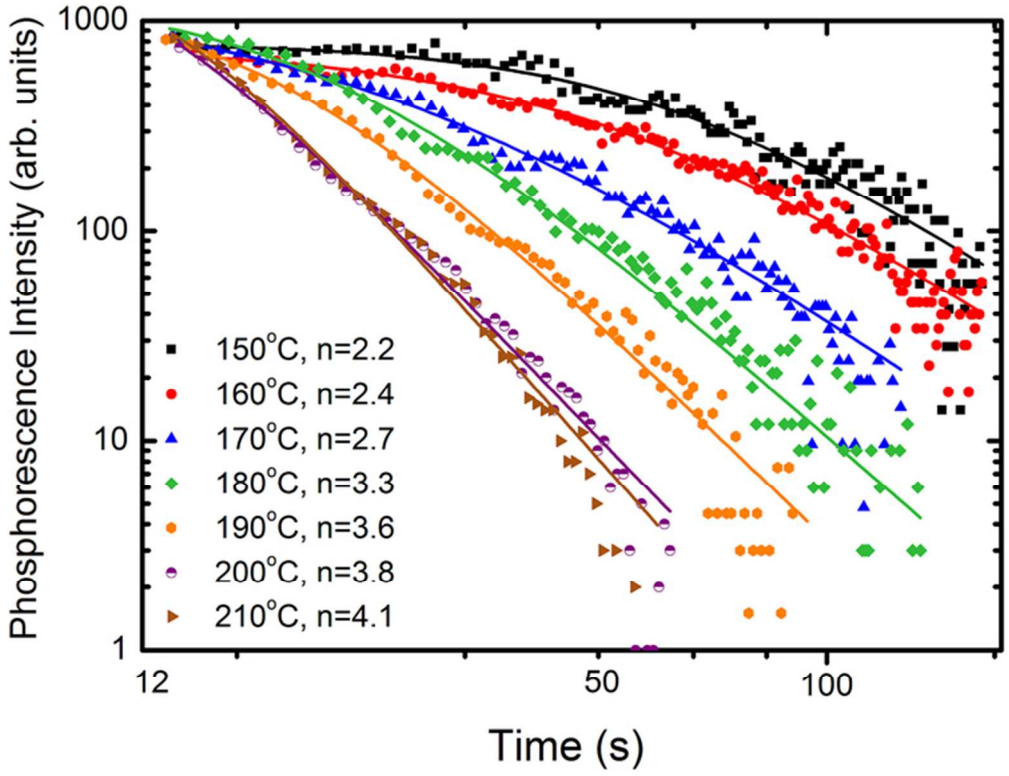

63x48mm (300 x 300 DPI)

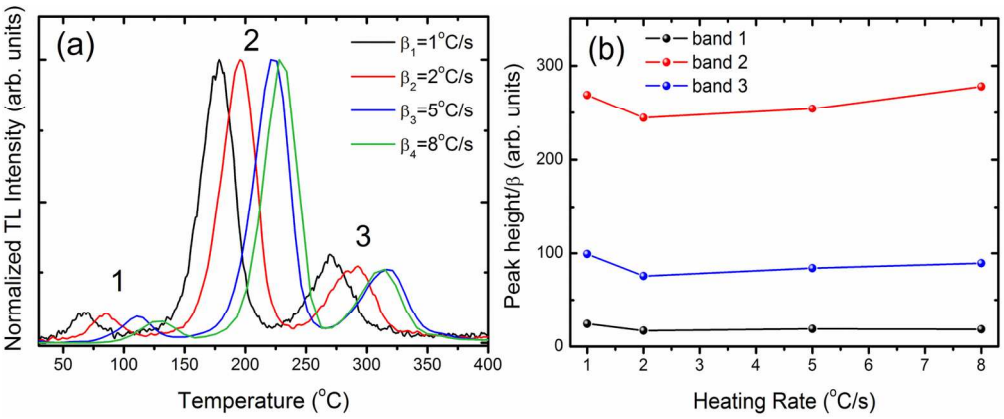

160x65mm (300 x 300 DPI)

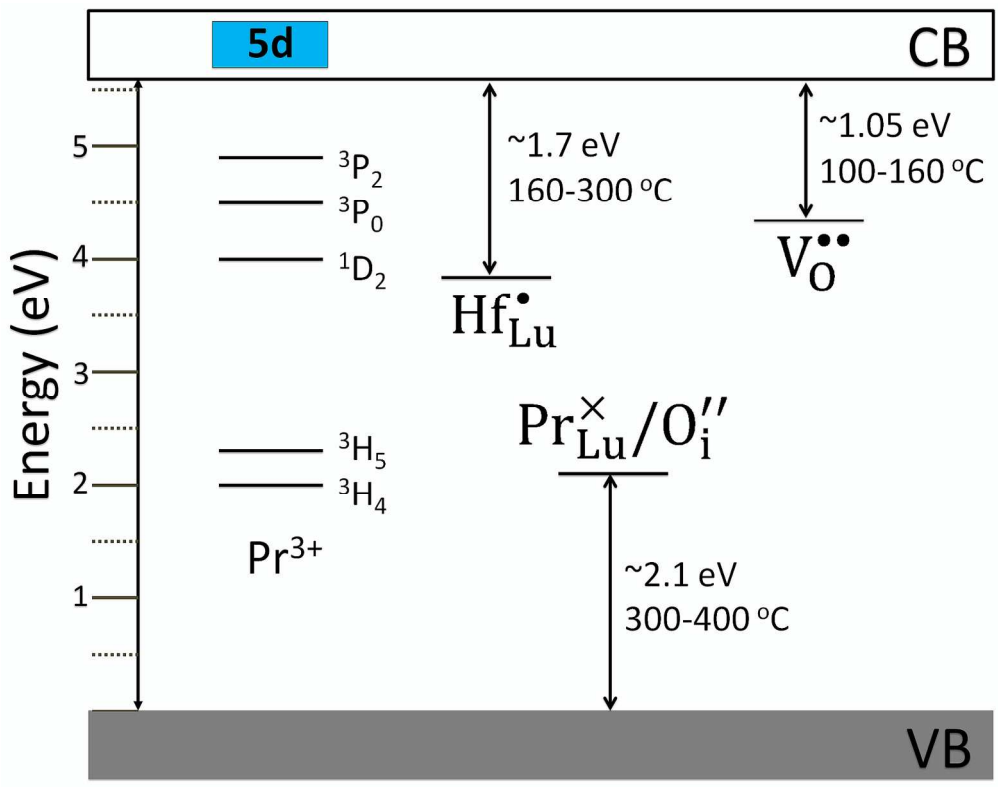

687x539mm (72 x 72 DPI)

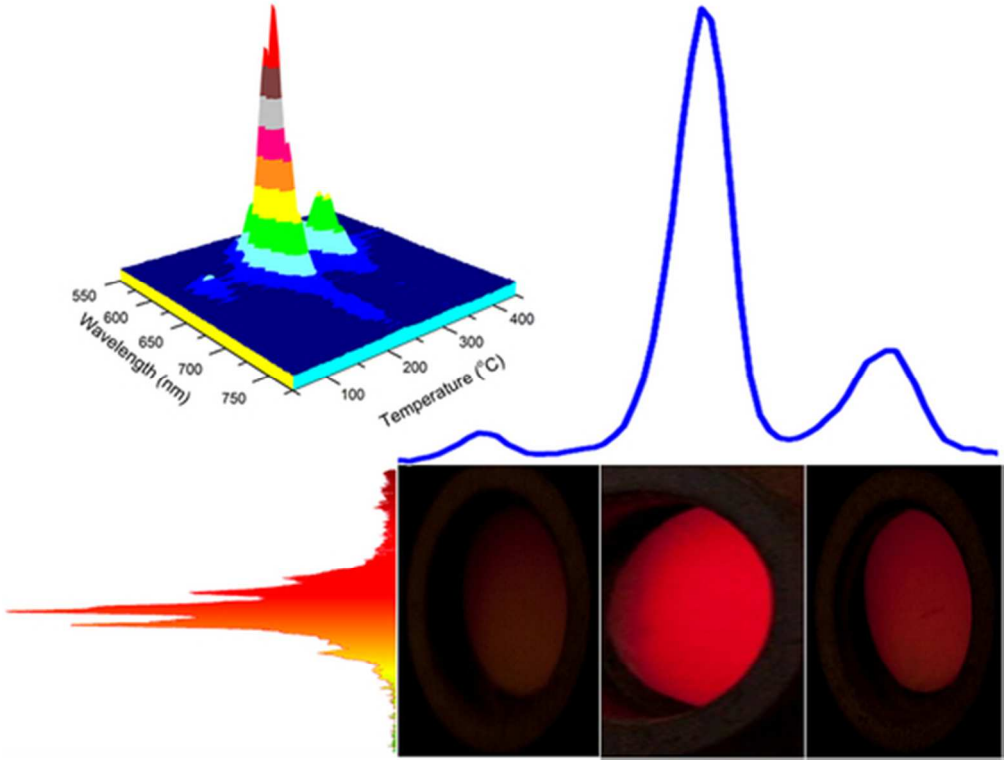

44x34mm (300 x 300 DPI)